wieland

Dr.-Ing. Robert Zauter, Dr. rer. nat. Frank Sperka, Peter Stahl

Forming Behavior of Hot-dip Tin Coatings

Published in the proceedings of the GMM-Fachtagung

GMM VDE/VDI-GESELLSCHAFT MIKROELEKTRONIK, MIKROSYSTEM- UND FEINWERKTECHNIK

VDI VDE

TH OWL TECHNISCHE HOCHSCHULE OSTWESTFALEN-LIPPE UNIVERSITY OF APPLIED SCIENCES AND ARTS

Forming Behavior of Hot-dip Tin Coatings

Dr.-Ing. Robert Zauter, Peter Stahl, Dr. rer. nat. Frank Sperka
Wieland-Werke AG
Graf-Arco-Str. 36, 89079 Ulm, Germany

Keywords: strip, copper, copper alloy, connector, tin, coating, hot-dip tin, tin layer, forming, strain, adhesion.

1. Introduction

To ensure the best possible electrical contact in a connector, the current-conducting copper materials must be coated with a metallic coating. Tin is used as a coating material for the transmission of signals and moderately high currents. Often hot-dip tin coatings are used which are economically attractive. During the production of the connector by stamping-bending processes, both the copper base material and the tin coating undergo considerable plastic forming, such as bending, coining/embossing and straining. While the forming behavior of the copper base materials is well known and can be calculated using FEA, the microstructural processes in hot-dip tin coatings during forming have hardly been investigated so far.

2. Microstructure of hot-dip tinned coatings

During the hot-dip tin coating process, the copper material in the form of wide strip is guided through a bath of molten tin, see schematic diagram in Fig. 1. The thickness of the tin layer is constant over the entire width and length of the strip. It is controlled by a hot air blow-off device and continuous layer thickness measurement. Thus, tin coatings can be produced in thickness intervals from 1-2 µm up to 10-20 µm. Miniaturized connectors usually consist of thin strip with strip thicknesses of ≤ 0.2 mm and tin coatings with low layer thicknesses in the range 0.8-2, 1-2 and 2-4 µm.

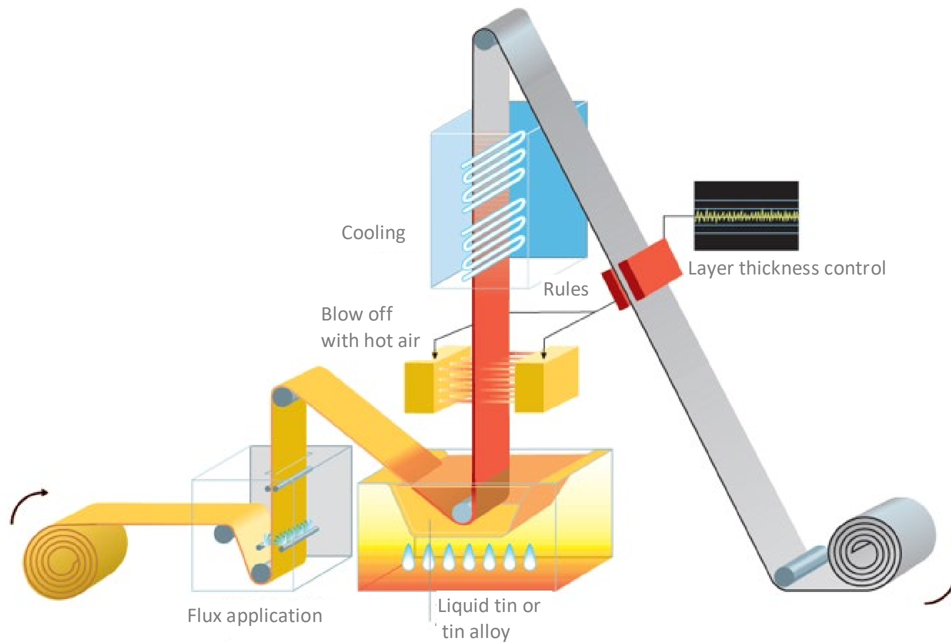

Figure 1: Schematic drawing of a hot-dip tinning line [1]. The use of hot air levelling and layer thickness control is state of the art today.

During the coating process, the strip for a short time is in contact with the liquid tin at a temperature slightly above the melting point of tin (232 °C). This results in spontaneous formation of an intermetallic phase (IMP) consisting of Cu and Sn on the surface of the strip in a thickness of about 0.5 µm. If the base material is a pure copper, both, the copper-rich ε-phase (Cu_3Sn) and the tin-rich η-phase (Cu_6Sn_5) form. In copper alloys, the ε-phase often is only very slightly pronounced or absent. A tin layer applied by hot-dip tinning exhibits typical properties which are described in DIN EN 13148 [2], e.g. visible crystallization phenomena and very good adhesion.

It is state of the art that different strip materials show different IMP growth characteristics and thus a different IMP morphology [3]. On phosphor bronze, the IMP grains grow parallel with round interfaces to the pure tin. In CuNiSi materials, the growth of the IMP grains is rod-like and takes place in multiple directions, see Fig. 2. Fig. 3 shows the corresponding microstructures in a cross-section.

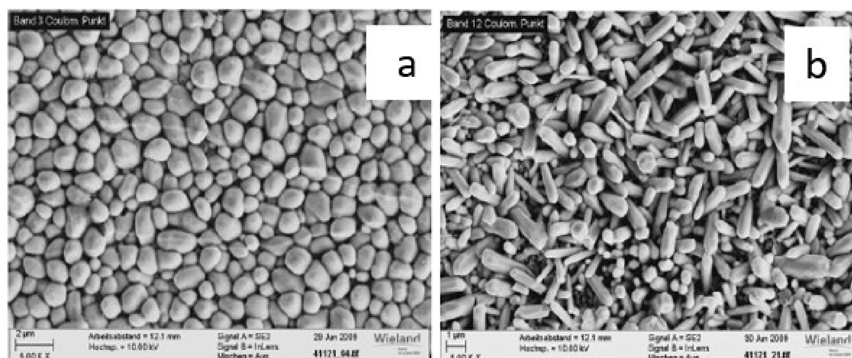

Figure 2: Top view of the intermetallic phase from which the pure tin was previously chemically removed. The different structure of the IMP can be seen, for a) bronze CuSn6, C51900, Wieland-B16 and b) CuNi3SiMg, C70250, Wieland-K55. This figure was published earlier in [3].

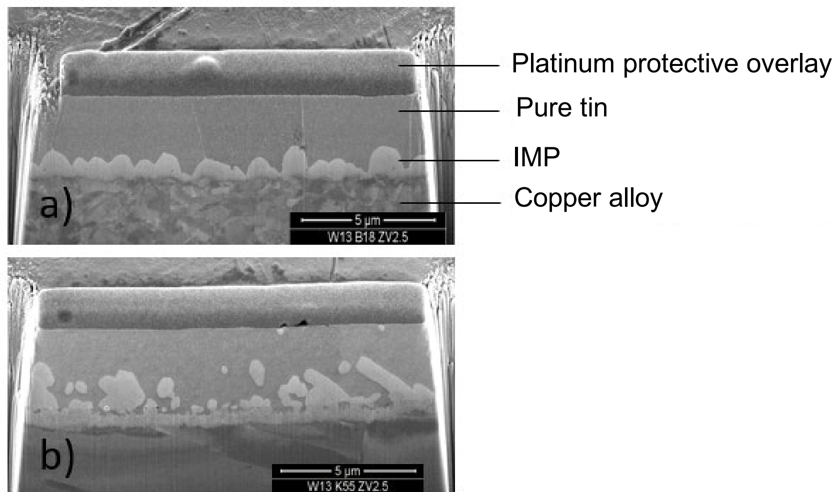

Figure 3: Cross-sections through the tin layer, generated by means of Focused Ion Beam (FIB) and imaged in the scanning electron microscope (SEM). Different characteristics of IMP on different base materials, a) bronze CuSn8 fine grain variant (C52100, Wieland-B18 SUPRALLOY®) and b) CuNi3SiMg (C70250, Wieland-K55). Similar micrographs have been published previously in [4].

In contrast to the ductile copper base materials and the pure tin in the tin layer, the intermetallic phase is brittle. When mechanical strain is applied, the IMP does not exhibit plastic deformation, but tends to crack.

3. Copper materials and tin coatings used in this study

In this study, high-strength materials with thin pure tin layers were selected that are typical for miniaturized connectors. These types of connectors are often used at elevated temperatures and are thus subject to the risk of diffusion-induced pore formation (Kirkendall pores). The following coated strip materials were used:

- CuSn8 fine-grain phosphor bronze, C52100, Wieland-B18 SUPRALLOY®,
  Temper R685, strip thickness 0.15 mm
  Hot-dip tin coating SnPUR® (pure tin) 1-2 µm

- CuNi3SiMg, C70250, Wieland-K55,
  Temper R620, strip thickness 0.15 mm
  Hot-dip tin coating SnPUR® (pure tin) 1-2 µm

- CuNi1ZnSi, C19005, Wieland-K73,
  Temper R580, strip thickness 0.20 mm
  Hot-dip tin coating SnPUR® (pure tin) 2-4 µm

4. Test performance

Strip specimens of the above materials were plastically strained in tensile tests and bulge tests. Tensile tests were stopped after defined plastic elongation of 2.5 %, 5.0 %, 7.5 % and 10 %. Above 10 % plastic strain the base material during tensile testing is susceptible to necking and strain becomes to occur only locally. Therefore, additional bulge tests were performed. Due to the nearly ideal biaxial stress state, higher plastic strains can be realized with this test method. In CuNi alloys plastic strain up to > 20 % for CuNiSi strip and up to > 30 % for phosphor bronze strip can be achieved, see Fig. 4b.

Samples were taken parallel to the direction of elongation, so that the photographic images of the microstructure reveal the elongation effects in the microstructure. The locations of the specimens are shown in Fig. 4a for the tensile tests (a separate test is required for each plastic strain) and Fig. 4b for the bulge tests. Several specimens with different plastic strains can be taken simultaneously from one bulge test. Each specimen was prepared by FIB and examined by SEM. The FIB sections allow the visualization of an approximately 15 µm long section of the coating in very high resolution and without artifacts that often occur with mechanical polishing. This makes it possible to show all kinds of cavities and pores as black areas, even if their size is very small.

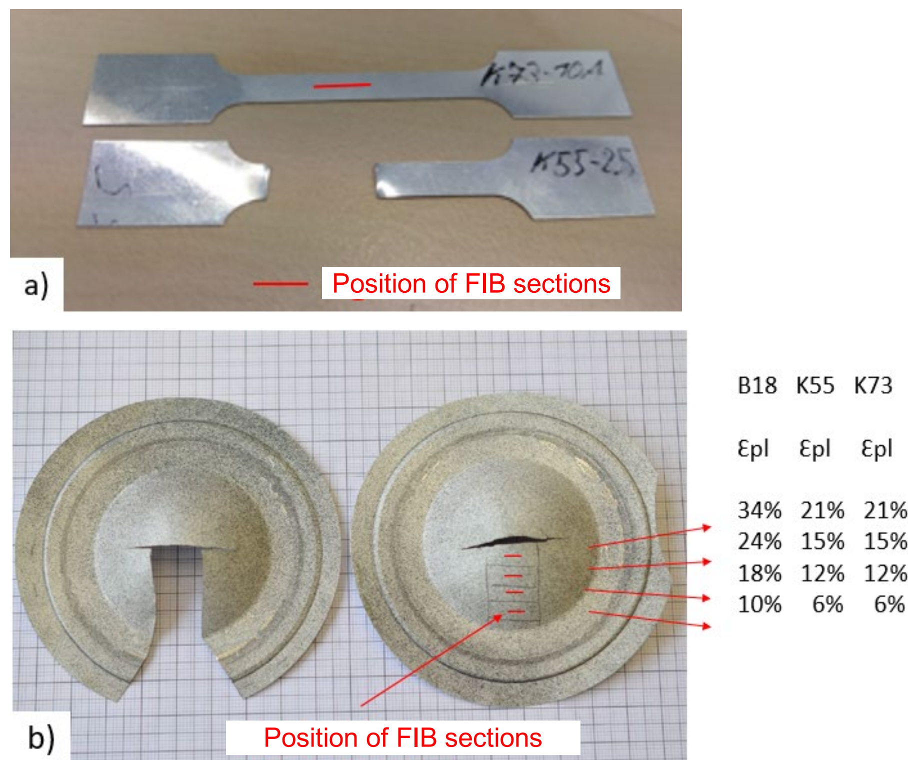

Figure 4: a) Tensile test specimens and the location of the FIB sections, b) Bulge test specimens, location of the FIB sections and the corresponding plastic strains.

For quantitative analysis of voids and pores, the SEM images were converted into black-and-white contrast by means of an image processing program. The solid material (copper base material, IMP and pure tin) appears white while voids/pores appear black. A reference area of 13.3 x 2.5 µm² = 33.25 µm² including the IMP (Fig. 5) was defined and identically applied to each micrograph. The selected resolution was 800 x 150 pixels, i.e. 3610 pixels/µm². The result of the evaluation is the sum of the void/pore area in % of the reference area.

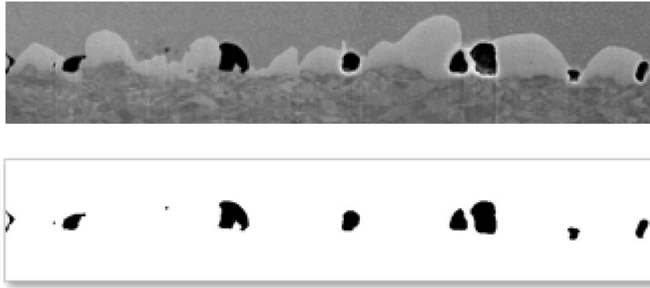

Figure 5: SEM image (above) and black-and-white contrast (below) of the reference area of size 13.3 x 2.5 µm². The reference area contains parts of the base material and the pure tin as well as the IMP and the IMP cracks.

5. Results

5.1 Tensile tests

The SEM images of the FIB sections in Fig. 6 show the microstructure of the tin layer, consisting of pure tin and IMP, as well as a small area of the base material. Each column represents one copper alloy according to the designation in the title line. From top to bottom, the applied plastic strain increases.

At a plastic strain value of ε_{pl} = 2.5 %, no cracks appear in the IMPs. On the copper base materials the first cracks become visible at ε_{pl} = 5 %, located at the grain boundaries of IMP grains - in the following referred to as IMP cracks. Starting at ε_{pl} = 7.5 %, the IMP cracks appear on the phosphor bronze as well. CuNiSi alloys and phosphor bronze thus show a different threshold value of plastic strain above which IMP cracks occur. This difference can be explained by the different structure of IMP described in Chapter 2, Fig. 2. With increasing plastic strain, the number of IMP cracks increases, which is clearly visible in the IMP on CuNiSi materials.

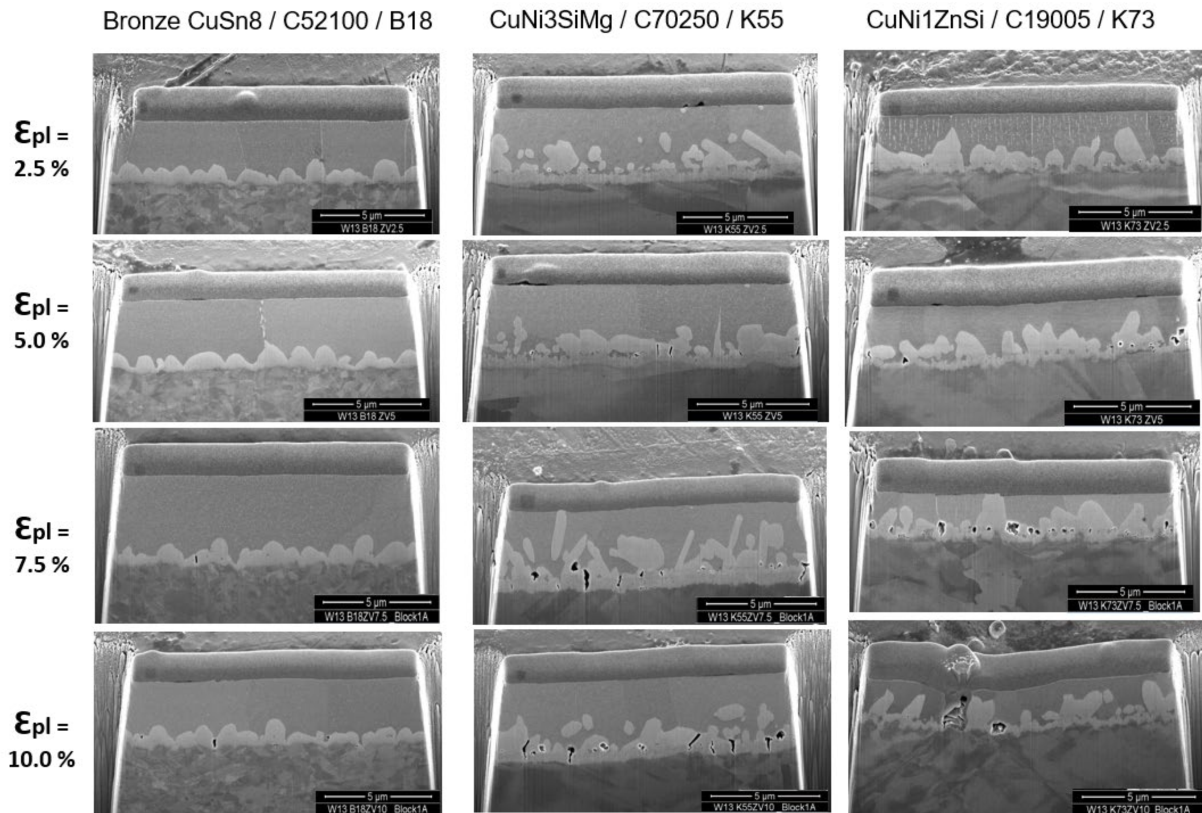

Figure 6: FIB-SEM images of tensile test specimens stopped at defined plastic strains. IMP cracks occur above a threshold level of plastic strain and their number increases with increasing plastic strain.

5.2 Bulge tests

In bulge test specimens considerably higher plastic strains can be obtained. The achievable strains depend on the base material. Fig. 7 shows the microstructure of the tin layers as a function of plastic strain for the fine-grain phosphor bronze CuSn8 (B18 SUPRALLOY®) and the CuNi3SiMg material (K55).

For both base materials, the number of IMP cracks increases with increasing plastic strain until almost every grain boundary is ruptured. At the same time, further elongation causes the existing cracks to increase in width.

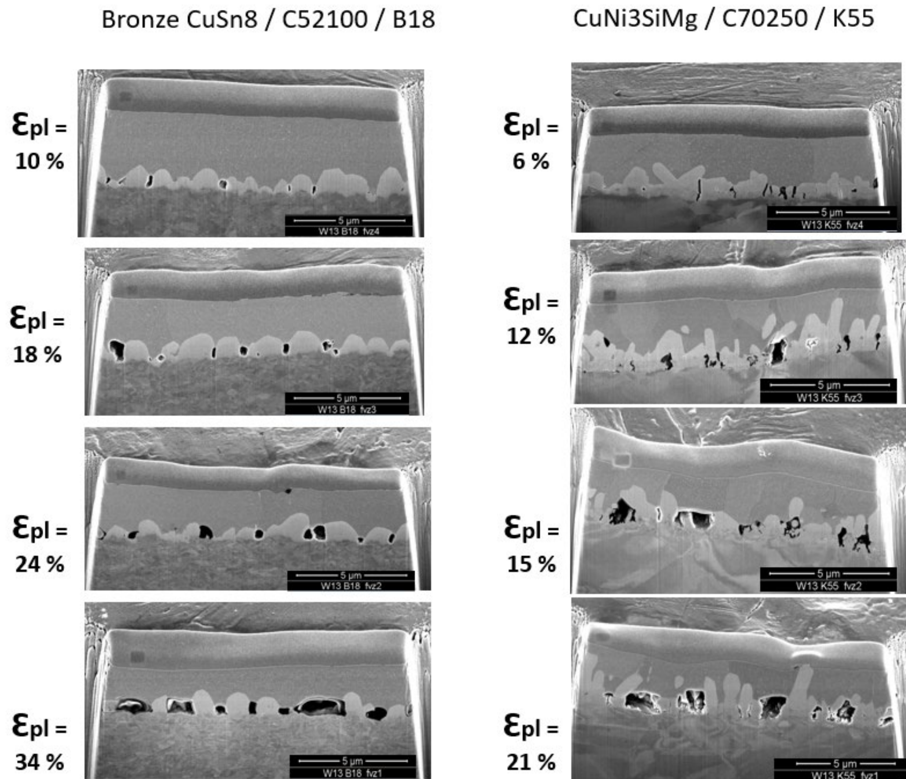

Figure 7: FIB-SEM images of the bulge test specimens taken at different plastic strains. With increasing plastic strain, the number of IMP cracks increases until almost all grain boundaries are ruptured. At the same time, the width of the IMP cracks increases. Shown are the phosphor bronze CuSn8 (C52100, Wieland-B18 SUPRALLOY®) and the CuNi3SiMg alloy (C70250, Wieland-K55).

Quantitative evaluation of the void/porosity areas provides an overall picture of the extent of strain-induced IMP cracking. Fig. 8 shows a plot of the ratio of void area in % of the reference area versus plastic strain. Based on the phenomenological information from the SEM images and the plot in Fig. 8, the following conclusions can be drawn:

1. The intermetallic phase withstands plastic strains without cracking up to a threshold value. At higher strains, cracks appear. This threshold value depends on the base material. First IMP-cracks were observed at values of plastic strain of
   5 % for both CuNiSi materials,
   7.5 % for the fine grain phosphor bronze CuSn8.
2. With increasing elongation, the number of IMP cracks increases until all IMP grain boundaries are ruptured.
3. At the same time, the IMP cracks widen with increasing plastic strain.
4. The IMP on the CuNiSi materials is more susceptible to cracking, resulting in a higher void volume even at smaller plastic compared to the phosphor bronze.

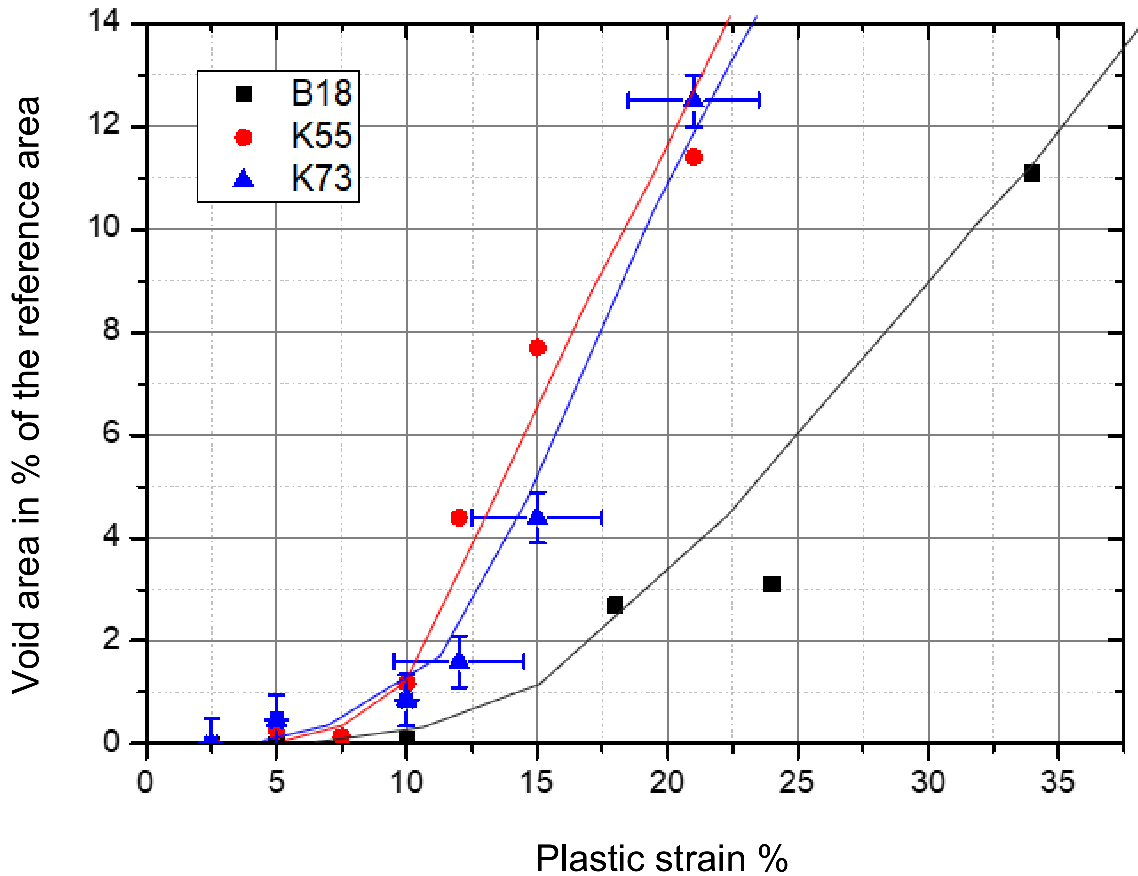

Fig. 8: Plot of total void area as a percentage of the reference area versus plastic strain. Note: Error bars were only plotted for C19005 (K73). For the other two materials, C70250 (K55) and CuSn8 (B18), they are of the same order of magnitude but not included into this diagram.

6. Application of the results to real connectors

The presence of curves describing pore area fractions as a function of applied plastic strain allows estimation of the amount of plastic strain in real components, e.g. in a contact tip of a miniaturized connector. An experimental tool for imprinting such contact tips was kindly provided by TE Connectivity. With this, tips were fabricated from two of the three test materials. FIB sections were produced and examined in the SEM from three regions which are differently deformed: a) the contact tip, b) the flank and c) undeformed material (see Fig. 9). The appearance of the voids is shown in Fig. 10. The quantitative estimation of the plastic strain is shown in Table 1.

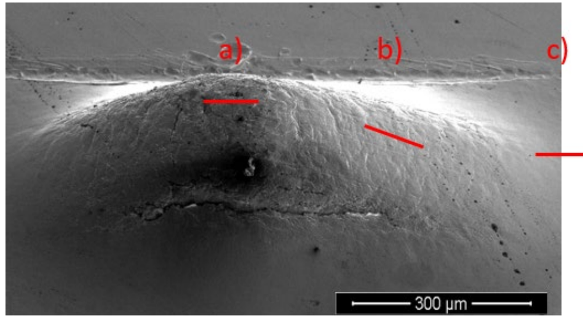

Figure 9: Contact tip produced with an embossing tool from TE Connectivity. The red lines indicate the position of the FIB sections at the positions a) contact tip, b) flank and c) undeformed material.

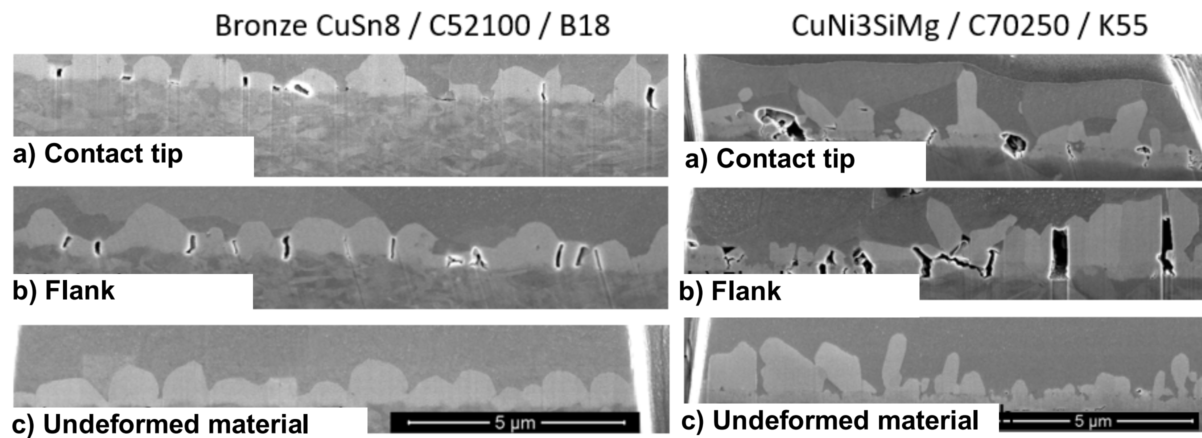

Figure 10: Formation of IMP cracks in three differently deformed areas on two different base materials: phosphor bronze (left) and CuNi3SiMg (right).

Table 1:
Quantitative estimation of the plastic strains which are present in different areas, derived from the pore images in Fig. 10 and the graph in Fig. 8.

Cu-material	Area	Void area fraction (%), measured	ε_{pl} (%), estimated from Fig. 8
CuSn8	Contact tip	0.5	12.0
CuSn8	Flank	0.7	12.5
CuSn8	Undeformed material	0	0
CuNi3SiMg	Contact tip	5.2	14.0
CuNi3SiMg	Flank	4.2	13.0
CuNi3SiMg	Undeformed material	0	0

7. Layer adhesion in the presence of IMP cracks

7.1 Layer adhesion after the stamping-bending process

During the manufacturing process of a connector by stamping-bending processes, strains of the base material and the tin layer take place in comparable orders of magnitude to those applied in this study via defined tests.

Without exception, the micrographs shown in Chapters 5 and 6 demonstrate very good adhesion of the IMP to the base metal. There is no material separation between the IMP and the base material in either the bronze or the CuNiSi alloys. Also, no progression of the IMP cracks into the neighboring material is discernible. Thus, neither the pure tin "above" the IMP nor the base material "below" the IMP show any damage or material separations parallel to the interfaces.

The excellent adhesion of the IMP to the base material is not surprising. Millions and millions of connectors are produced daily by stamping-bending processes of hot-dip tinned strips without any delamination being observed. Subsequently, the connectors are in operation for many years without any problems and without layer delamination.

7.2 Layer adhesion after service at elevated temperature (> 100 °C)

In the automotive industry, service temperatures of > 100 °C are frequently defined for miniaturized connectors. This raises further questions.

a) Which base materials/copper alloys are suitable?

On the one hand, the base materials must provide sufficient resistance to thermal stress relaxation. A decrease of strength of 10 to 15 % is considered acceptable. Tin bronzes reach this level of thermal stress relaxation at 105°C / 1000 h. If service temperatures become higher, CuNiSi alloys have to be applied. At 120 °C / 1000 h CuNiSi alloys relax about 10 %.

Secondly, the materials must provide good coating adhesion. In CuNiSi certain concentrations of alloying elements are capable of decelerate the diffusion of copper atoms into the tin layer. This limits the formation of diffusion pores – also known as Kirkendall pores - to a tolerable level and ensures a sufficiently good tin layer adhesion at elevated service temperatures over longer periods [5]. CuNi1ZnSi (C19005, Wieland-K73) and CuNi3SiMg (C70250, Wieland-K55) are both considered suitable in this respect.

b) Interaction of IMP cracks and Kirkendall pores

The question arises whether IMP cracks and Kirkendall pores, which develop at elevated temperature, interact and whether the interaction reduces the coating adhesion. For this purpose, annealing of strained strip specimens at 105 °C for 1000 h was performed. FIB-SEM microsections were investigated. As a first result it became obvious that IMP cracks after annealing are smaller in size compared to the unannealed material. This would be equivalent to a healing effect of the IMP cracks under temperature.

To verify this healing effect, annealing (105 °C, 1000 h) was performed on the specimens that already contained FIB sections. Subsequently, the existing FIB sections were reinserted into the FIB and freshly prepared, i.e. the oxide layer was carefully removed. The subsequent SEM images thus show the same location as before annealing. The image planes differ by only a few nanometers. Figs. 11 and 12 show

the arrangement of the IMP cracks due to annealing in a comparative view on CuNi3SiMg alloy and on CuSn8 bronze, respectively.

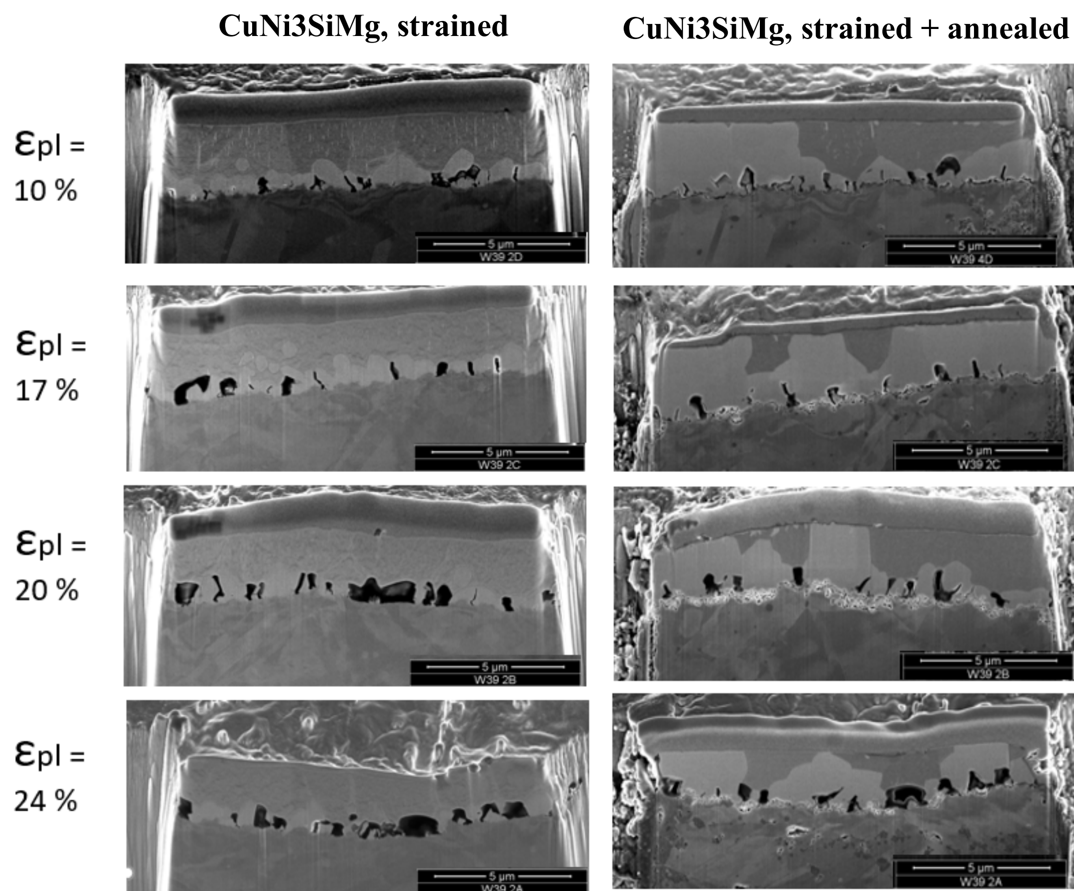

Figure 11, base material CuNi3SiMg: Comparison of the IMP crack arrangement before (left column) and after annealing (right column), each created on the same FIB cut position. The decrease in number and size of IMP cracks is recognizable. Thus, it can be assumed that the IMP cracks on CuNi3SiMg formed by plastic strain heal during thermal treatment at 105 °C for 1000 h.

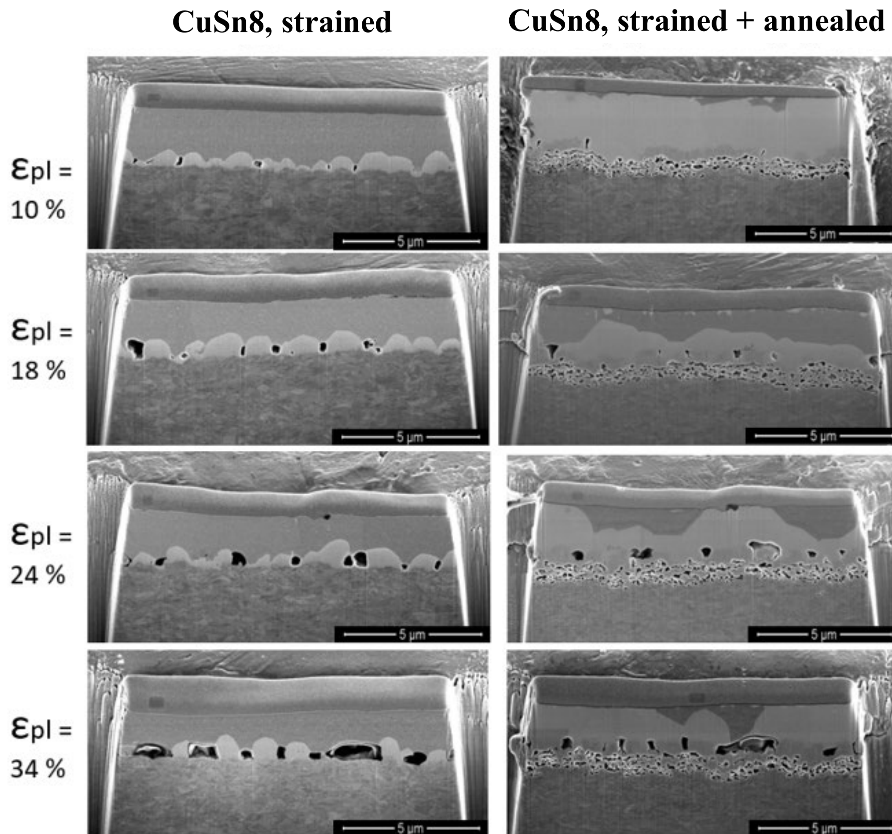

Figure 12, base material CuSn8: Comparison of the IMP crack arrangement before (left column) and after annealing (right column), each created on the same FIB cut position. The decrease in number and size of IMP cracks is recognizable. Thus, it can be assumed that the IMP cracks on CuSn8 formed by plastic strain heal during thermal treatment at 105 °C for 1000 h.

The following conclusions can be drawn from this investigation:

- The IMP cracks do not grow further under temperature exposure at > 100 °C. On the contrary, they show a tendency to heal.
- The Kirkendall pores are not formed in the plane where the IMP cracks are located, but one level below in the base material from which the diffusing copper atoms originally came from.
- The IMP continues to grow into the pure tin and surrounds the IMP cracks.
- Delamination of IMP and base material does not occur.
- An interaction of IMP cracks and Kirkendall pores with regards to reduction of tin layer adhesion is not evident.

8. Conclusion

IMP cracks in hot-dip tin coated strip are created during the production of connectors by stamping-bending processes. The IMP cracks are strain-induced. Crack initiation and expansion differs slightly in dependence of the base material. In this study, one bronze and two CuNiSi alloys were investigated, which all are materials commonly used in miniaturized connectors and applied at elevated operating temperatures (> 100 °C). The IMP cracks start at a plastic strain threshold of 5 and 7.5 % (CuNiSi materials and bronze, respectively) and become more in number and wider in extension with increasing strain. Strain-induced IMP cracks are considered harmless for several reasons:

1. After production, the tin layer around the IMP cracks exhibits excellent adhesion to the copper base material.
2. During use at elevated operating temperature (> 100 °C), the strain-induced IMP cracks do not grow further. On the contrary, IMP cracks tend to heal due to diffusion processes.
3. An interaction of IMP cracks and Kirkendall pores with regards to reduction of tin layer adhesion is not evident. Both effects are located at different planes.

9. Literature

[1] Wieland-Werke AG, product brochure "Hot-dip tinned copper and copper-alloy strip", revision Oct. 2022.
[2] DIN EN 13148:2010, German Institute for Standardization, Dec. 2010.
[3] I. Buresch, Effects of intermetallic phases on the properties of tin surfaces on copper alloys, 21st Albert-Keil Contact Seminar, Karlsruhe, Sept. 28-30, 2011, VDE-Verlag.
[4] H. Schmidt, I. Buresch, and A. Stokowski, Aging mechanisms in connectors that do not follow Arrhenius correlations, 25th Albert-Keil Contact Seminar, Karlsruhe, Oct. 09-11, 2019, VDE-Verlag.
[5] European patent specification EP 1288321 B1, 2002/2005.

wieland

Wieland-Werke AG | Graf-Arco-Straße 36 | 89079 Ulm | Germany
info@wieland.com | wieland.com

Diese Drucksache unterliegt keinem Änderungsdienst. Abgesehen von Vorsatz oder grober Fahrlässigkeit übernehmen wir für ihre inhaltliche Richtigkeit keine Haftung.
Die Produkteigenschaften gelten als nicht zugesichert und ersetzen keine Beratung durch unsere Experten.

03/2023 RP.TMA/Zr